

# Electrostatic dust-acoustic envelope solitons in an electron depleted plasma

R.K. Shikha<sup>\*,1</sup>, N.A. Chowdhury<sup>\*\*,2</sup>, A. Mannan<sup>‡1,3</sup>, and A.A. Mamun<sup>§,1</sup>

<sup>1</sup>*Department of Physics, Jahangirnagar University, Savar, Dhaka-1342, Bangladesh*

<sup>2</sup>*Plasma Physics Division, Atomic Energy Centre, Dhaka-1000, Bangladesh*

<sup>3</sup>*Institut für Mathematik, Martin Luther Universität Halle-Wittenberg, Halle, Germany*

*e-mail: \*shikha261phy@gmail.com, \*\*nurealam1743phy@gmail.com,*

*‡abdulmannan@juniv.edu, §mamun\_phys@juniv.edu*

---

## Abstract

A standard nonlinear Schrödinger equation has been established by using the reductive perturbation method to investigate the propagation of electrostatic dust-acoustic waves, and their modulational instability as well as the formation of localized electrostatic envelope solitons in an electron depleted unmagnetized dusty plasma system comprising opposite polarity dust grains and super-thermal positive ions. The relevant physical plasma parameters (viz., charge, mass, number density of positive and negative dust grains, and super-thermality of the positive ions, etc.) have rigorous impact to recognize the stability conditions of dust-acoustic waves. The present study is useful for understanding the mechanism of the formation of dust-acoustic envelope solitons associated with dust-acoustic waves in the laboratory and space environments.

---

## 1. Introduction

The research regarding opposite polarity dusty plasma, which is the combination of electrons, ions, and highly charged opposite polarity dust grains (DGs), has been increased tremendously due to their existence in astrophysical environments (viz., asteroid zones [1], interstellar clouds [1], planetary rings [2], Jupiter's magnetosphere [3], cometary tails [3], Earth polar mesosphere [3], and solar system [4], etc.) and laboratory observation [5, 6]. When energetic plasma particles (electrons or ions) are incident onto a DG surface, they are either backscattered/reflected by the DG or they pass through the DG material. During their passage they may lose their energy partially or fully. A portion of the lost energy can go into exciting other electrons that in turn may escape from the material. The emitted electrons are known as secondary electrons. The release of these secondary electrons from the DG tends to make the grain surface positive [7]. The interaction of photons incident onto the DG surface causes photoemission of electrons from the DG surface. The DGs, which emit photoelectrons, may become positively charged [7]. The emitted electrons collide with other DGs and are captured by some of these grains which may become negatively charged [7]. There are, of course, a number of other DG charging mechanisms, namely thermionic emission, field emission, and impact ionization, etc.

The process by which electrons are inserted to the negatively charged massive DGs from the background of the dusty plasma medium (DPM) is known as electron depletion, and this electron depleted plasma (EDP) can be observed in interstellar clouds [1], cometary tails [3],

Earth polar mesosphere [3], Jupiter's magnetosphere [3], solar system [4], F-rings of Saturn [8], and laboratory observation [5, 6]. Shukla and Silin [2] considered inertial ions and immobile DGs to investigate dust-ion-acoustic (DIA) waves (DIAWs) in an EDP. Sahu and Tribeche [8] studied dust-acoustic (DA) shock waves (DASHWs) and DA solitary waves (DASWs) in non-planer geometry. Mamun *et al.* [9] analyzed electrostatic solitary potential structures in an EDP, and reported that the existence of large number of ion and DG causes to increase the amplitude of the negative potentials. Ferdousi *et al.* [10] examined the DASHWs by considering a two-component EDP, and demonstrated that under consideration both negative and positive potential structures can exist. Borhanian and Shahmansouri [11] considered a three-component DPM having inertial massive negative DGs and inertialess two temperature ions, and investigated DASWs in presence of two temperature super-thermal ions, and highlighted that the phase velocity increases with ion population but decreases with ion temperature. Mayout and Tribeche [12] theoretically analyzed DA double-layers (DADLs) in an EDP, and graphically recognized that the amplitude of the DADLs causes to decrease with super-thermality of the plasma species. Sahu and Tribeche [13] studied small amplitude DADLs in a two-component non-thermal EDP.

The parameter  $\kappa$  in super-thermal/ $\kappa$ -distribution can describe the deviation (due to the presence of long range force fields) of the plasma species from the Maxwellian distribution [14, 15, 16, 17, 18]. The  $\kappa$ -distribution behaves as Maxwellian distribution for large values of  $\kappa$  (i.e.,  $\kappa \rightarrow \infty$ ) [15, 16, 17, 18]. Panwar *et al.* [15] demonstrated a theoretical investigation regarding the propagation of ion-acoustic waves (IAWs) in a three-component plasma having super-thermal electrons, and found that the amplitude of the compressive (rarefactive) cnoidal waves increases (decreases) with super-thermality of the electrons. Eslami *et al.* [16] analyzed DIAWs in presence of super-thermal plasma species, and reported that the speed of the DIAWs increases with the increase in the value of the super-thermality of the plasma species. Younsi and Tribeche [17] examined the effects of excess super-thermal electrons on the formation of electron-acoustic waves (EAWs) in a three-component plasma medium. Saini and Singh [18] studied head on collision of two DIAWs in a multi-component super-thermal plasma, and observed that both amplitude and width of the profile are increasing with  $\kappa$ .

The nonlinear Schrödinger equation (NLSE) is one of the eye-catching equations which can describe the modulational instability (MI) of various kinds of waves, viz., EAWs [19], IAWs [20], DIAWs [21], and DA waves (DAWs) [22], etc. Sultana and Kourakis [19] studied the MI of the EAWs and associated bright and dark envelope solitons in a three-component super-thermal plasma. Gharaee *et al.* [20] examined the stability criteria of the IAWs in presence of the super-thermal electrons. Jukui and He [21] theoretically analyzed the MI conditions of the cylindrical and spherical DIAWs. Gill *et al.* [22] considered inertial positive and negative DGs and inertialess electrons and ions to study the MI of the DAWs in a multi-component plasma medium, and reported that the critical wave number which determines the modulationally stable and unstable domains of the DAWs decreases with increasing the value of  $\kappa$ . Borhanian *et al.* [23] numerically examined electromagnetic envelope solitons in magnetized plasma and found that solitons (bright or dark-type) propagate in the magnetized plasma without any change in amplitude and shape. In this paper, our aim is to investigate the MI criteria of DAWs and associated envelope solitons in a three-component EDP having inertial positive and negative DGs and inertialess  $\kappa$ -distributed ions.

The manuscript is organized as follows: The governing equations are provided in section 2. The derivation of the NLSE by using the reductive perturbation method (RPM) is demonstrated in section 3. The MI of DAWs is presented in section 4. The envelope solitons are presented in section 5. The conclusion is shown in section 6.

## 2. Governing Equations

We consider a three-component unmagnetized EDP comprising inertial negatively and positively charged massive DGs, and  $\kappa$ -distributed positive ions. At equilibrium, the quasi-neutrality condition can be written as  $Z_i n_{i0} + Z_+ n_{+0} \approx Z_- n_{-0}$ ; where  $n_{i0}$  is the number densities of positive ions, and  $n_{-0}$  ( $n_{+0}$ ) is the number densities of negative (positive) DGs;  $Z_i$  is the charge state of positive ions, and  $Z_-$  ( $Z_+$ ) is the charge state of negative (positive) DGs. So, the normalizing equations for our plasma model can be written as

$$\frac{\partial n_-}{\partial t} + \frac{\partial}{\partial x}(n_- u_-) = 0, \quad (1)$$

$$\frac{\partial u_-}{\partial t} + u_- \frac{\partial u_-}{\partial x} + \beta_1 n_- \frac{\partial n_-}{\partial x} = \frac{\partial \phi}{\partial x}, \quad (2)$$

$$\frac{\partial n_+}{\partial t} + \frac{\partial}{\partial x}(n_+ u_+) = 0, \quad (3)$$

$$\frac{\partial u_+}{\partial t} + u_+ \frac{\partial u_+}{\partial x} + \beta_2 n_+ \frac{\partial n_+}{\partial x} = -\beta_3 \frac{\partial \phi}{\partial x}, \quad (4)$$

$$\frac{\partial^2 \phi}{\partial x^2} = n_- - (1 - \beta_4) n_i - \beta_4 n_+, \quad (5)$$

where  $n_i$ ,  $n_-$ , and  $n_+$  are normalized by  $n_{i0}$ ,  $n_{-0}$ , and  $n_{+0}$ , respectively;  $u_+$  ( $u_-$ ) represents the positive (negative) dust fluid speed which is normalized by the DA wave speed  $C_- = (Z_- k_B T_i / m_-)^{1/2}$  (with  $T_i$  being temperature of ion,  $m_+$  being positive dust mass, and  $k_B$  being the Boltzmann constant);  $\phi$  represents the electrostatic wave potential normalized by  $k_B T_i / e$  (with  $e$  being the magnitude of single electron charge); the time and space variables are, respectively, normalized by  $\omega_p^-^{-1} = (m_- / 4\pi e^2 Z_-^2 n_{-0})^{1/2}$  and  $\lambda_{D_-} = (k_B T_i / 4\pi e^2 Z_- n_{-0})^{1/2}$ .  $P_- = P_{-0} (N_- / n_{-0})^\gamma$  (with  $P_{-0}$  being the equilibrium pressure term of the negative DGs),  $P_+ = P_{+0} (N_+ / n_{+0})^\gamma$  (with  $P_{+0}$  being the equilibrium pressure term of the positive DGs), and  $\gamma = (N + 2) / N$ , where  $N$  is the degree of freedom and for one-dimensional case  $N = 1$ , then  $\gamma = 3$ ;  $P_{-0} = n_{-0} k_B T_-$ ,  $P_{+0} = n_{+0} k_B T_+$  (with  $T_-$  and  $T_+$  being the temperature of negative and positive DGs); and other parameters are  $\beta_1 = 3T_- / Z_- T_i$ ,  $\beta_2 = 3T_+ m_- / Z_- T_i m_+$ ,  $\beta_3 = Z_+ m_- / Z_- m_+$ , and  $\beta_4 = Z_+ n_{+0} / Z_- n_{-0}$ . It may be noted here that we have considered  $m_- > m_+$ ,  $Z_- > Z_+$ , and  $n_{-0} > n_{+0}$ . The expression for the number density of ions following the  $\kappa$ -distribution [6] can be written as

$$n_i = \left[ 1 + \frac{\phi}{(\kappa - 3/2)} \right]^{-\kappa + \frac{1}{2}} \quad (6)$$

where the parameter  $\kappa$  is known as super-thermality of the positive ions. Now, by substituting Eq. (6) into Eq. (5), and expanding the term  $\phi$  up to third order, we obtain

$$\frac{\partial^2 \phi}{\partial x^2} + \beta_4 n_+ = (\beta_4 - 1) + n_- + G_1 \phi + G_2 \phi^2 + G_3 \phi^3 + \dots, \quad (7)$$

where

$$G_1 = \frac{(1 - \beta_4)(2\kappa - 1)}{(2\kappa - 3)}, \quad G_2 = -\frac{(1 - \beta_4)(2\kappa - 1)(2\kappa + 1)}{2(2\kappa - 3)^2},$$

$$G_3 = \frac{(1 - \beta_4)(2\kappa - 1)(2\kappa + 1)(2\kappa + 3)}{6(2\kappa - 3)^3}.$$

### 3. Derivation of the NLSE

To study the MI of DAWs, we will derive the NLSE by employing the RPM. So, we first introduce the stretched co-ordinates [24, 25, 26, 27, 28, 29]

$$\xi = \epsilon(x - v_g t), \quad (8)$$

$$\tau = \epsilon^2 t, \quad (9)$$

where  $v_g$  is the group speed and  $\epsilon$  is a small parameter. Then, we can write the dependent variables as

$$n_- = 1 + \sum_{m=1}^{\infty} \epsilon^m \sum_{l=-\infty}^{\infty} n_{-l}^{(m)}(\xi, \tau) \exp[il(kx - \omega t)], \quad (10)$$

$$u_- = \sum_{m=1}^{\infty} \epsilon^m \sum_{l=-\infty}^{\infty} u_{-l}^{(m)}(\xi, \tau) \exp[il(kx - \omega t)], \quad (11)$$

$$n_+ = 1 + \sum_{m=1}^{\infty} \epsilon^m \sum_{l=-\infty}^{\infty} n_{+l}^{(m)}(\xi, \tau) \exp[il(kx - \omega t)], \quad (12)$$

$$u_+ = \sum_{m=1}^{\infty} \epsilon^m \sum_{l=-\infty}^{\infty} u_{+l}^{(m)}(\xi, \tau) \exp[il(kx - \omega t)], \quad (13)$$

$$\phi = \sum_{m=1}^{\infty} \epsilon^m \sum_{l=-\infty}^{\infty} \phi_l^{(m)}(\xi, \tau) \exp[il(kx - \omega t)], \quad (14)$$

where  $k$  ( $\omega$ ) is real variable representing the carrier wave number (frequency). The derivative operators in the above equations are treated as follows [30, 31, 32, 33, 34, 35, 36]:

$$\frac{\partial}{\partial t} \rightarrow \frac{\partial}{\partial t} - \epsilon v_g \frac{\partial}{\partial \xi} + \epsilon^2 \frac{\partial}{\partial \tau}, \quad (15)$$

$$\frac{\partial}{\partial x} \rightarrow \frac{\partial}{\partial x} + \epsilon \frac{\partial}{\partial \xi}. \quad (16)$$

Now, by substituting Eqs. (10)–(16) into Eqs. (1)–(4) and Eq. (7), and collecting the terms containing  $\epsilon$ , the first order ( $m = 1$  with  $l = 1$ ) equations can be expressed as

$$\omega n_{-1}^{(1)} = k u_{-1}^{(1)}, \quad (17)$$

$$k \phi_1^{(1)} = k \beta_1 n_{-1}^{(1)} - \omega u_{-1}^{(1)}, \quad (18)$$

$$\omega n_{+1}^{(1)} = k u_{+1}^{(1)}, \quad (19)$$

$$k \beta_3 \phi_1^{(1)} = \omega u_{+1}^{(1)} - k \beta_2 n_{+1}^{(1)}, \quad (20)$$

$$n_{-1}^{(1)} = \beta_4 n_{+1}^{(1)} - k^2 \phi_1^{(1)} - G_1 \phi_1^{(1)}, \quad (21)$$

these equations reduce to

$$n_{-1}^{(1)} = \frac{k^2}{M} \phi_1^{(1)}, \quad (22)$$

$$u_{-1}^{(1)} = \frac{\omega k}{M} \phi_1^{(1)}, \quad (23)$$

$$n_{+1}^{(1)} = \frac{\beta_3 k^2}{N} \phi_1^{(1)}, \quad (24)$$

$$u_{+1}^{(1)} = \frac{\omega k \beta_3}{N} \phi_1^{(1)}, \quad (25)$$

where  $M = \beta_1 k^2 - \omega^2$  and  $N = \omega^2 - \beta_2 k^2$ . We thus obtain the dispersion relation of DAWs

$$\omega^2 = \frac{k^2 T \pm k^2 \sqrt{T^2 - 4(G_1 + k^2)L}}{2(G_1 + k^2)}, \quad (26)$$

where  $L = \beta_2 + \beta_1 \beta_2 G_1 + \beta_1 \beta_3 \beta_4 + \beta_1 \beta_2 k^2$  and  $T = 1 + \beta_1 G_1 + \beta_2 G_1 + \beta_3 \beta_4 + \beta_1 k^2 + \beta_2 k^2$ . In Eq. (26), to get real and positive values of  $\omega$ , the condition  $T^2 > 4(G_1 + k^2)L$  should be satisfied. The positive and negative signs in Eq. (26) corresponds to the fast ( $\omega_f$ ) and slow ( $\omega_s$ ) DA modes. The fast DA mode corresponds to the case in which both inertial DGs oscillate in phase with the inertialess ions. On the other hand, the slow DA mode corresponds to the case in which only one of the inertial DGs oscillates in phase with inertialess ions, but the other inertial DG in anti-phase with them [37, 38]. The second-order ( $m = 2$  with  $l = 1$ ) equations are given by

$$n_{-1}^{(2)} = \frac{k^2}{M} \phi_1^{(2)} + \frac{i(k\omega^2 - 2v_g \omega k^2 - kM + \beta_1 k^3)}{M^2} \frac{\partial \phi_1^{(1)}}{\partial \xi}, \quad (27)$$

$$u_{-1}^{(2)} = \frac{k\omega}{M} \phi_1^{(2)} + \frac{i(\omega^3 + \beta_1 \omega k^2 - 2v_g k \omega^2 - v_g k M)}{M^2} \frac{\partial \phi_1^{(1)}}{\partial \xi}, \quad (28)$$

$$n_{+1}^{(2)} = \frac{\beta_3 k^2}{N} \phi_1^{(2)} - \frac{i\beta_3(\beta_2 k^3 - 2\omega v_g k^2 + k\omega^2 + kN)}{N^2} \frac{\partial \phi_1^{(1)}}{\partial \xi}, \quad (29)$$

$$u_{+1}^{(2)} = \frac{\beta_3 k \omega}{N} \phi_1^{(2)} - \frac{i\beta_3(\beta_2 \omega k^2 - 2v_g k \omega^2 + v_g k N + \omega^3)}{N^2} \frac{\partial \phi_1^{(1)}}{\partial \xi}, \quad (30)$$

with compatibility condition, we can find the group velocity

$$v_g = \frac{k^2(\beta_1 N^2 + \beta_2 \beta_3 \beta_4 M^2) + \omega^2(N^2 + \beta_3 \beta_4 M^2) - 2M^2 N^2 - MN(N - \beta_3 \beta_4 M)}{2\omega k(N^2 + \beta_3 \beta_4 M^2)}. \quad (31)$$

The coefficients of  $\epsilon$  for  $m = 2$  with  $l = 2$  provide the second order harmonic amplitudes which are found to be proportional to  $|\phi_1^{(1)}|^2$

$$n_{-2}^{(2)} = G_4 |\phi_1^{(1)}|^2, \quad (32)$$

$$u_{-2}^{(2)} = G_5 |\phi_1^{(1)}|^2, \quad (33)$$

$$n_{+2}^{(2)} = G_6 |\phi_1^{(1)}|^2, \quad (34)$$

$$u_{+2}^{(2)} = G_7 |\phi_1^{(1)}|^2, \quad (35)$$

$$\phi_2^{(2)} = G_8 |\phi_1^{(1)}|^2, \quad (36)$$

where

$$\begin{aligned}
G_4 &= \frac{2G_8k^2M^2 - (3\omega^2k^4 + \beta_1k^6)}{2M^3}, \\
G_5 &= \frac{\omega G_4M^2 - \omega k^4}{kM^2}, \\
G_6 &= \frac{2\beta_3G_8k^2N^2 + 3\omega^2\beta_3^2k^4 + \beta_2\beta_3^2k^6}{2N^3}, \\
G_7 &= \frac{\omega G_6N^2 - \omega\beta_3^2k^4}{kN^2}, \\
G_8 &= \frac{N^3(3\omega^2k^4 + \beta_1k^6) + \beta_4M^3(3\omega^2\beta_3^2k^4 + \beta_2\beta_3^2k^6) - 2G_2M^3N^3}{2M^2k^2N^3 + 2M^3N^3(4k^2 + G_1) - 2\beta_3\beta_4N^2k^2M^3}.
\end{aligned}$$

Now, we consider the expression for ( $m = 3$  with  $l = 0$ ) and ( $m = 2$  with  $l = 0$ ) which leads to the zeroth harmonic modes. Thus, we obtain

$$n_{-0}^{(2)} = G_9|\phi_1^{(1)}|^2, \quad (37)$$

$$u_{-0}^{(2)} = G_{10}|\phi_1^{(1)}|^2, \quad (38)$$

$$n_{+0}^{(2)} = G_{11}|\phi_1^{(1)}|^2, \quad (39)$$

$$u_{+0}^{(2)} = G_{12}|\phi_1^{(1)}|^2, \quad (40)$$

$$\phi_0^{(2)} = G_{13}|\phi_1^{(1)}|^2, \quad (41)$$

where

$$\begin{aligned}
G_9 &= \frac{\beta_1k^4 + \omega^2k^2 + 2v_g\omega k^3 - G_{13}M^2}{M^2(v_g^2 - \beta_1)}, \\
G_{10} &= \frac{v_gG_9M^2 - 2\omega k^3}{M^2}, \\
G_{11} &= \frac{2v_g\omega\beta_3^2k^3 + \omega^2k^2\beta_3^2 + \beta_2\beta_3^2k^4 + \beta_3G_{13}N^2}{N^2(v_g^2 - \beta_2)}, \\
G_{12} &= \frac{v_gG_{11}N^2 - 2\omega\beta_3^2k^3}{N^2}, \\
G_{13} &= \frac{N^2(2v_g\omega k^3 + \beta_1k^4 + k^2\omega^2)(v_g^2 - \beta_2) + 2G_2M^2N^2(v_g^2 - \beta_1)(v_g^2 - \beta_2) - \mathcal{S}_1}{\beta_3\beta_4M^2N^2(v_g^2 - \beta_1) + M^2N^2(v_g^2 - \beta_2) - \mathcal{S}_2}.
\end{aligned}$$

where  $\mathcal{S}_1 = \beta_4M^2(2v_g\omega\beta_3^2k^3 + \beta_2\beta_3^2k^4 + \beta_3^2k^2\omega^2)(v_g^2 - \beta_1)$  and  $\mathcal{S}_2 = G_1M^2N^2(v_g^2 - \beta_1)(v_g^2 - \beta_2)$ . Finally, the third harmonic modes ( $m = 3$ ) and ( $l = 1$ ), with the help of Eqs. (22)–(41), give a set of equations which can be reduced to the following NLSE:

$$i\frac{\partial\Phi}{\partial\tau} + P\frac{\partial^2\Phi}{\partial\xi^2} + Q|\Phi|^2\Phi = 0, \quad (42)$$

where  $\Phi = \phi_1^{(1)}$  is used for simplicity. The dispersion coefficient  $P$  is

$$P = \frac{N^3\{(v_g\omega - \beta_1k)(\beta_1k^3 - 2v_g\omega k^2 + k\omega^2 - kM) + (v_gk - \omega)(\beta_1\omega k^2 - 2v_gk\omega^2 + \omega^3 - v_gkM)\} - \mathcal{S}_3}{2\omega k^2MN(N^2 + \beta_3\beta_4M^2)},$$

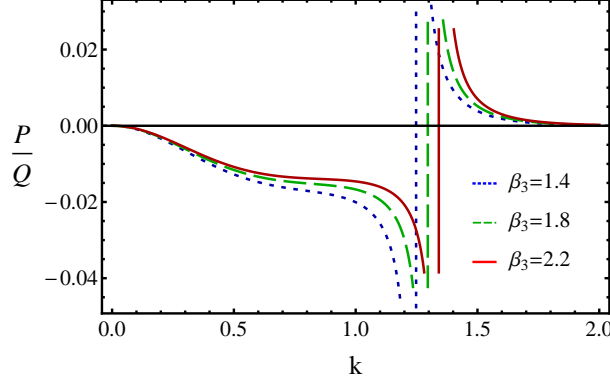


Figure 1: Plot of  $P/Q$  vs  $k$  for different values of  $\beta_3$  when  $\beta_1 = 0.006$ ,  $\beta_2 = 0.06$ ,  $\beta_4 = 0.8$ ,  $\kappa = 1.7$ , and  $\omega_f$ .

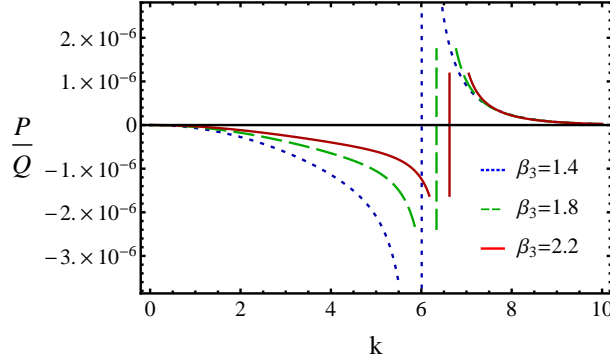


Figure 2: Plot of  $P/Q$  vs  $k$  for different values of  $\beta_3$  when  $\beta_1 = 0.006$ ,  $\beta_2 = 0.06$ ,  $\beta_4 = 0.8$ ,  $\kappa = 1.7$ , and  $\omega_s$ .

where  $\mathcal{S}_3 = M^3 N^3 + \beta_3 \beta_4 M^3 \{(v_g k - \omega)(\beta_2 \omega k^2 - 2v_g k \omega^2 + \omega^3 + v_g k N) - (v_g \omega - \beta_2 k)(\beta_2 k^3 - 2\omega v_g k^2 + k \omega^2 + k N)\}$  and the nonlinear coefficient  $Q$  is

$$Q = \frac{2G_2 M^2 N^2 (G_8 + G_{13}) + 3G_3 M^2 N^2 - 2\omega N^2 k^3 (G_5 + G_{10}) - 2\omega \beta_3 \beta_4 M^2 k^3 (G_7 + G_{12}) - \mathcal{S}_4}{2\omega k^2 (N^2 + \beta_3 \beta_4 M^2)},$$

where  $\mathcal{S}_4 = N^2 (\omega^2 k^2 + \beta_1 k^4) (G_4 + G_9) + M^2 (\beta_3 \beta_4 \omega^2 k^2 + \beta_2 \beta_3 \beta_4 k^4) (G_6 + G_{11})$ . It may be noted here that both  $P$  and  $Q$  are functions of various plasma parameters such as  $k$ ,  $\beta_3$ ,  $\beta_4$ , and  $\kappa$ . So, all the plasma parameters are used to maintain the nonlinearity and the dispersion properties of the EDP.

#### 4. Modulational instability

The space and time evolution of the DAWs in an EDP medium are directly governed by the dispersion ( $P$ ) and nonlinear ( $Q$ ) coefficients of NLSE, and are indirectly governed by different plasma parameters such as  $k$ ,  $\beta_3$ ,  $\beta_4$ , and  $\kappa$ . Thus, these plasma parameters significantly

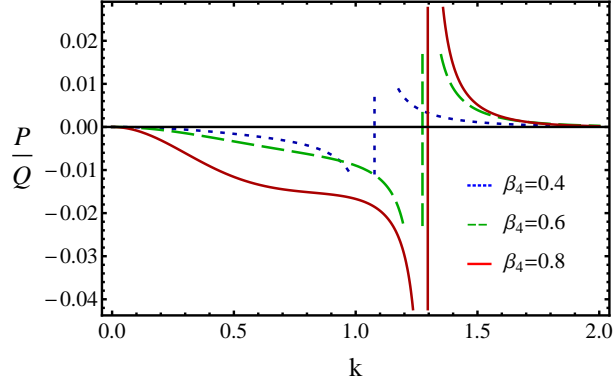


Figure 3: Plot of  $P/Q$  vs  $k$  for different values of  $\beta_4$  when  $\beta_1 = 0.006, \beta_2 = 0.06, \beta_3 = 1.8, \kappa = 1.7$ , and  $\omega_f$ .

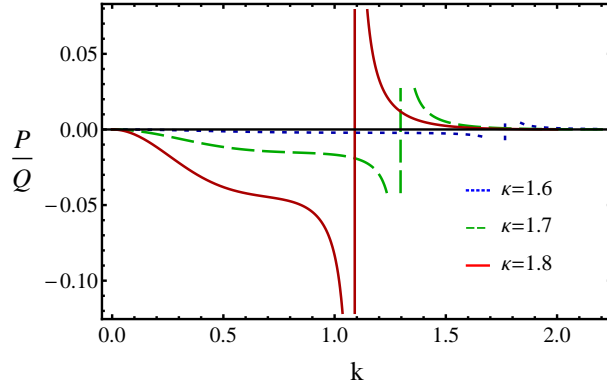


Figure 4: Plot of  $P/Q$  vs  $k$  for different values of  $\kappa$  when  $\beta_1 = 0.006, \beta_2 = 0.06, \beta_3 = 1.8, \beta_4 = 0.8$ , and  $\omega_f$ .

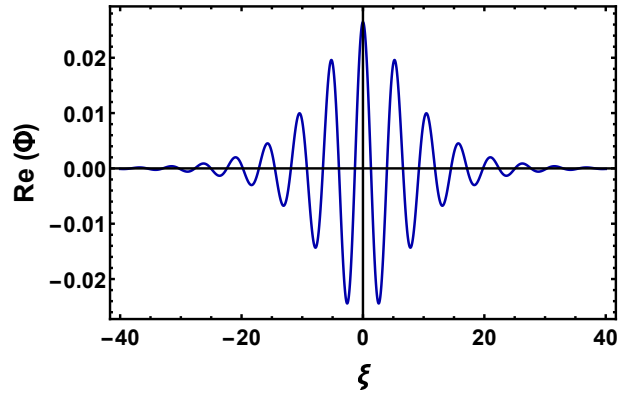


Figure 5: The variation of  $Re(\Phi)$  vs  $\xi$  for bright envelope solitons when  $k = 1.4, \tau = 0, \beta_1 = 0.006, \beta_2 = 0.06, \beta_3 = 1.8, \beta_4 = 0.8, \psi_0 = 0.0007, \tau = 0, U = 0.5, \Omega_0 = 0.2, \kappa = 1.7$ , and  $\omega_f$ .

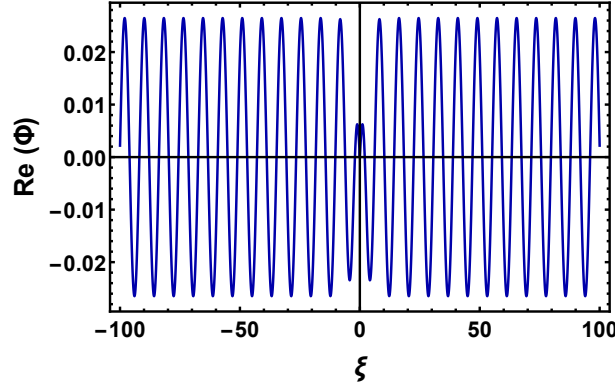


Figure 6: The variation of  $Re(\Phi)$  vs  $\xi$  for dark envelope solitons when  $k = 0.2$ ,  $\tau = 0$ ,  $\beta_1 = 0.006$ ,  $\beta_2 = 0.06$ ,  $\beta_3 = 1.8$ ,  $\beta_4 = 0.8$ ,  $\psi_0 = 0.0007$ ,  $\tau = 0$ ,  $U = 0.5$ ,  $\Omega_0 = 0.2$ ,  $\kappa = 1.7$ , and  $\omega_f$ .

change the stability conditions of DAWs. The stable and unstable parametric regimes of DAWs are organised by the sign of  $P$  and  $Q$  of Eq. (42) [19, 20, 21, 22]. When  $P$  and  $Q$  have the same sign (i.e.,  $P/Q > 0$ ), the evolution of DAWs amplitude is modulationally unstable in the presence of external perturbations, and allows to generate bright envelope solitons. On the other hand, when  $P$  and  $Q$  have opposite signs (i.e.,  $P/Q < 0$ ), the evolution of DAWs amplitude is modulationally stable in the presence of external perturbations, and allows to generate dark envelope solitons. The plot of  $P/Q$  against  $k$  yields stable and unstable parametric regimes of the DAWs. The point, at which the transition of  $P/Q$  curve intersects with the  $k$ -axis, is known as the threshold or critical wave number  $k (= k_c)$  [19, 20, 21, 22].

We have investigated the stable/unstable parametric regimes for the DAWs by depicting  $P/Q$  versus  $k$  graph for different values of  $\beta_3$  in Fig. 1 (under the consideration of fast mode) and in Fig. 2 (under the consideration of slow mode). It is clear from these figures that (a) for both fast and slow modes, DAWs are modulationally stable (i.e.,  $P$  and  $Q$  have opposite sign) and unstable (i.e.,  $P$  and  $Q$  have same sign) for small values of  $k$ ; (b) the  $k_c$  increases with an increase in the value of  $\beta_3$ ; (c) the charge state of the negative dust ( $Z_-$ ) reduces the  $k_c$  as well as destabilize the DAWs for small values of  $k$  while the charge state of the positive dust ( $Z_+$ ) increases the  $k_c$  as well as destabilize the DAWs for large values of  $k$  when their masses remain constant; (d) in fast mode, DAWs are modulationally unstable for small value of  $k$  ( $k \cong 1.2$ ) while in slow mode, DAWs are modulationally unstable for large value of  $k$  ( $k \cong 6.0$ ) with respect to the fast mode when other plasma parameters remain constant.

Figure 3 describes the effects of the number density of the positive and negative dust grains and their charge state in recognizing the stable and unstable regions of the DAWs. It is clear from this figure that (a) as we increase  $\beta_4$ , the  $k_c$  increases as well as destabilize the DAWs for large values of  $k$ ; (b) the increase in the value of the positive (negative) dust grains number density causes to increase (decrease) the  $k_c$  for a constant value of positive and negative dust grains charge state (via  $\beta_4$ ). The super-thermal ions of EDP can easily demonstrate the stability criterion of the DAWs, and it is obvious from Fig. 4 that as we increase the value of  $\kappa$ , the  $k_c$  decreases as well as destabilize the DAWs for small values of  $k$ .

## 5. Envelope solitons

The envelope solitonic solutions of the NLSE (42), which can be obtained by a number of straightforward mathematical steps, are available in a large number of existing literature [19]. The bright envelope solitons corresponding to the unstable parametric regime (i.e.,  $P/Q > 0$ ) can be written as

$$\Phi(\xi, \tau) = \left[ \psi_0 \operatorname{sech}^2 \left( \frac{\xi - U\tau}{W} \right) \right]^{1/2} \times \exp \left[ \frac{i}{2P} \left\{ U\xi + \left( \Omega_0 - \frac{U^2}{2} \right) \tau \right\} \right], \quad (43)$$

where  $\psi_0$  is the amplitude of localized pulse for both bright and dark envelope soliton,  $U$  is the propagation speed of the localized pulse,  $W$  is the soliton width, and  $\Omega_0$  is the oscillating frequency at  $U = 0$ . The soliton width  $W$  and the maximum amplitude  $\psi_0$  are related by  $W = \sqrt{2|P/Q|}/\psi_0$ . We have exhibited the bright envelope solitons in Fig. 5. On the other hand, the dark envelope solitons corresponding to the stable parametric regime (i.e.,  $P/Q < 0$ ) can be written as

$$\Phi(\xi, \tau) = \left[ \psi_0 \tanh^2 \left( \frac{\xi - U\tau}{W} \right) \right]^{1/2} \times \exp \left[ \frac{i}{2P} \left\{ U\xi - \left( \frac{U^2}{2} - 2PQ\psi_0 \right) \tau \right\} \right]. \quad (44)$$

We have exhibited the dark envelope solitons in Fig. 6.

## 6. Conclusion

In this paper, we have theoretically and numerically analysed the criteria of MI of DAWs and associated bright and dark envelope solitons in a three-component EDP having inertial positive and negative DGs and inertialess super-thermal electrons. We have employed RPM for deriving the NLSE. The EDP medium under consideration supports the stable and unstable DAWs depending on the sign of the ratio of  $P$  and  $Q$ . The relevant physical plasma parameters (viz., charge, mass, number density of positive and negative dust grains, and super-thermality of the ions) play an important role in recognizing the stability conditions as well as generation of the bright and dark electrostatic envelope solitons. It may be noted here that the effects of gravitational and the magnetic fields are very important but beyond the scope of our present work. In future and for better understanding, someone can investigate the nonlinear propagation in a three-component EDP by considering the effects of these gravitational and magnetic fields. The findings of our present investigation should be useful to understand the nonlinear phenomena (viz. MI and envelope solitons) in space plasma (i.e., interstellar clouds [1], cometary tails [3], and F-rings of Saturn [8], etc.) and laboratory experiments.

## acknowledgements

The authors are grateful to the anonymous reviewer for his/her constructive suggestions which have significantly improved the quality of our manuscript. A. Mannan thanks the Alexander von Humboldt Foundation for a Postdoctoral Fellowship.

## References

- [1] P. K. Shukla, Phys. Plasmas **8**, 1791 (2001).
- [2] P. K. Shukla and V. P. Silin, Phys. Scr. **45**, 508 (1992).
- [3] M. M. Hossen, M. S. Alam, S. Sultana, and A. A. Mamun, Eur. Phys. J. D **70**, 252 (2016).
- [4] M. M. Hossen, L. Nahar, M. S. Alam, S. Sultana, and A. A. Mamun, High Energ. Dens. Phys. **24**, 9 (2017).
- [5] A. Barkan, R. L. Merlino, and N. D'Angelo, Phys. Plasmas **2**, 3563 (1995).
- [6] M. Shahmansouri and H. Alinejad, Phys. Plasmas **20**, 033704 (2013).
- [7] P. K. Shukla and A. A. Mamun, Introduction to Dusty Plasma Physics, Institute of Physics, Bristol, 2002.
- [8] B. Sahu and M. Tribeche, Astrophys. Space Sci. **338**, 259 (2012).
- [9] A. A. Mamun, R. A. Cairns, and P. K. Shukla, Phys. Plasmas **3**, 702 (1996).
- [10] M. Ferdousi, M. R. Miah, S. Sultana, and A. A. Mamun, Astrophys. Space Sci. **43**, 360 (2015).
- [11] J. Borhanian and M. Shahmansouri, Phys. Plasmas **20**, 013707 (2013).
- [12] S. Mayout and M. Tribeche, J. Plasma Phys. **78**, 657 (2012).
- [13] B. Sahu and M. Tribeche, Astrophys. Space Sci. **341**, 573 (2012).
- [14] V. M. Vasylunas, J. Geophys. Res. **73**, 2839 (1968).
- [15] A. Panwar, C. M. Ryu, and A. S. Bains, Phys. Plasmas **21**, 122105 (2014).
- [16] P. Eslami, M. Mottaghizadeh, and H. R. Pakzad, IEEE Trans. Plasma Sci. **41**, 12 (2013).
- [17] S. Younsi and M. Tribeche, Astrophys. Space Sci. **330**, 295 (2010).
- [18] N. S. Saini and K. Singh, Phys. Plasmas **23**, 103701 (2016).
- [19] S. Sultana and I. Kourakis, Plasma Phys. Control. Fusion **53**, 045003 (2011).
- [20] H. Gharaee, S. Afghah, and H. Abbasi, Phys. Plasmas **18**, 032116 (2011).
- [21] X. Jukui and L. He, Phys. Plasmas **10** (2), 339 (2002).
- [22] T. S. Gill, A. S. Bains, and C. Bedi, Phys. Plasmas **17**, 013701 (2010).
- [23] J. Borhanian, I. Kourakis, and S. Sobhanian, Phys. Lett. A **373**, 3667 (2009).
- [24] N. A. Chowdhury, A. Mannan, M. M. Hasan, and A. A. Mamun, Chaos **27**, 093105 (2017).
- [25] N. A. Chowdhury, A. Mannan, and A. A. Mamun, Phys. plasmas **24**, 113701 (2017).
- [26] M. H. Rahman, N. A. Chowdhury, A. Mannan, M. Rahman, and A. A. Mamun, Chinese J. Phys. **56**, 2061 (2018).
- [27] M. H. Rahman, A. Mannan, N. A. Chowdhury, and A. A. Mamun, Phys. Plasmas **25**, 102118 (2018).
- [28] N. A. Chowdhury, A. Mannan, M. M. Hasan, and A. A. Mamun, Vacuum **147**, 31 (2018).
- [29] N. A. Chowdhury, A. Mannan, M. R. Hossen, and A. A. Mamun, Contrib. Plasma Phys. **58**, 870 (2018).
- [30] N. Ahmed, A. Mannan, N. A. Chowdhury, and A. A. Mamun, Chaos **28**, 123107 (2018).
- [31] N. A. Chowdhury, A. Mannan, M. M. Hasan, and A. A. Mamun, Plasma Phys. Rep. **45**, 459 (2019).
- [32] S. Jahan, N. A. Chowdhury, A. Mannan, and A. A. Mamun, Commun. Theor. Phys. **71**, 327 (2019).
- [33] M. Hassan, M. H. Rahman, N. A. Chowdhury, *et al.*, Commun. Theor. Phys. **71**, 1017 (2019).
- [34] R. K. Shikha, N. A. Chowdhury, A. Mannan, and A. A. Mamun, Eur. Phys. J. D **73**, 177 (2019).
- [35] S. Jahan, A. Mannan, N. A. Chowdhury, and A. A. Mamun, Plasma Phys. Rep. **46**, 90 (2020).
- [36] S. K. Paul, N. A. Chowdhury, A. Mannan, and A. A. Mamun, Pramana-J Phys **94**, 58 (2020).
- [37] A. E. Dubinov, Plasma Phys. Rep. **35**, 991 (2009).
- [38] E. Saberiana, A. Esfandyari-Kalejahib, and M. Afsari-Ghazib, Plasma Phys. Rep. **43**, 83 (2017).